THE JOURNAL OF PHYSICAL CHEMISTRY C

Article

pubs.acs.org/JPCC

Structural Properties of Picene–Perfluoropentacene and Picene–Pentacene Blends: Superlattice Formation versus Limited Intermixing

Johannes Dieterle,[†] Katharina Broch,[†,‡] Alexander Hinderhofer,[†] Heiko Frank,[†] Jiří Novák,[§] Alexander Gerlach,[†] Tobias Breuer,[∥] Rupak Banerjee,[†,⊥] Gregor Witte,[∥] and Frank Schreiber*[,†]

[†]Institut für Angewandte Physik, Universität Tübingen, Auf der Morgenstelle 10, 72076 Tübingen, Germany

[‡]Cavendish Laboratory, University of Cambridge, J. J. Thomson Avenue, CB3 0HE Cambridge, United Kingdom

[§]Central European Institute of Technology, Masaryk University, Kamenice 5, CZ-62500 Brno, Czech Republic

[∥]Fachbereich Physik, Philipps-Universität Marburg, Renthof 7, 35032 Marburg, Germany

[⊥]Department of Physics, Indian Institute of Technology Gandhinagar, Ahmedabad 382424, India

S Supporting Information

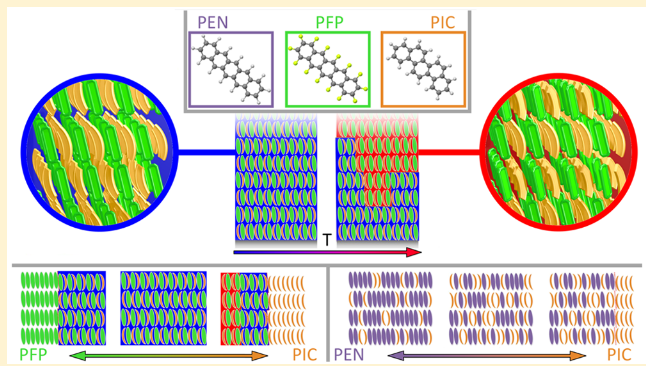

ABSTRACT: The structure and morphology of mixed thin films of picene ($C_{22}H_{14}$, PIC) and perfluoropentacene ($C_{22}F_{14}$, PFP) as well as mixed thin films of PIC and pentacene ($C_{22}H_{14}$, PEN) grown by simultaneous coevaporation is investigated using X-ray diffraction, atomic force microscopy, and near-edge X-ray absorption spectroscopy. For both systems we find mixing on the molecular level and the formation of mixed structures. However, due to the strongly different interactions in both mixtures the ordering is fundamentally different. For the equimolar PFP:PIC mixtures, we observe the formation of two different mixed polymorphs with unit cells containing 2 PIC and 2 PFP molecules depending on the growth temperature. One of these polymorphs is a superlattice with in-plane compound segregation. The other polymorph is less symmetric and results only in a very short ranged in-plane ordering. In contrast, the PEN:PIC mixtures form crystals with unit cell parameters continuously changing with the molar concentrations between those of the pure compounds. The position of molecular species within the crystal lattice is statistical. Surprisingly, for higher concentrations of PIC we observe phase separation of surplus PIC molecules which corresponds to a limited intermixing of the two compounds. Finally, the results are discussed in the context of other organic semiconductor binary mixtures showing that besides chemical composition and steric compatibility the intramolecular arrangement of the atoms important for intermolecular interactions significantly influences the structure formation in organic semiconductor blends.

■ INTRODUCTION

Mixtures of organic semiconductors (OSC) are relevant for numerous electronic and optoelectronic applications[1] such as organic field effect transistors,[2] organic light-emitting diodes,[3,4] and solar cells.[5,6] The optical and electronic properties in such mixed thin films strongly depend on the morphology and structural properties such as crystallinity and degree of intermixing.[7−11] The growth and structure formation of binary mixed thin film OSC systems are not yet well understood, and it is in fact already rather challenging to predict the structure of a single-component OSC thin film.[12]

There are several factors affecting the mixing and ordering behavior of binary OSC mixtures.[13,14] First, the intermolecular interaction energies W_{A-A}, W_{A-B}, and W_{B-B} in a mixture containing molecules of species A and B can lead to mixing or phase separation depending on the interplay of the interaction energies. Second, the steric compatibility, i.e., the relative size and shape of the compounds, is important. If the compounds differ significantly in size[15] or shape,[10] phase separation may be preferred. In contrast, entropy always favors intermixing.

In mixtures of aromatic molecules the intermolecular interactions are dominated by van der Waals and electrostatic forces, which are important for systems containing arenes and perfluorinated arenes.[16] In the latter mixtures, there is a strong attractive interaction between molecules of different species that in many cases leads to the formation of an equimolar ordered molecular mixture. For rodlike OSC a face-to-face stacking in alternating columnar arrangements is frequently

Received: September 11, 2015
Revised: October 26, 2015
Published: October 26, 2015

DOI: 10.1021/acs.jpcc.5b08866
J. Phys. Chem. C 2015, 119, 26339−26347

observed, e.g., arene−perfluoroarene stacking[16,17] and phenyl−perfluorophenyl stacking.[18,19] The formation of equimolar mixed structures was also found in mixed thin films of PFP and PEN[20] and in mixtures of PFP and diindenoperylene (DIP).[21]

For many mixed systems of rodlike OSCs such as PFP:PEN,[20] PFP:DIP,[21] and PEN:DIP[22] a mean field model treating molecules as cylinders with different in-plane and out-of-plane interaction parameters and taking into account sterical issues and chemical composition[22] can explain the mixing and ordering behavior. Here, we present a study of the impact of small changes in the molecular structure on the mixing and ordering behavior and structure formation. The organic superconductor PIC[23−25] is structurally quite similar to the benchmark organic semiconductor PEN[26−29] such that PIC and PEN share the same atomic composition and are both formed by five fused benzene rings. The only difference between both molecules is the arrangement of these rings which is linear in the case of PEN and staggered for PIC (see Figure 1a). PFP,[30−32] on the other hand, is sterically highly compatible with PEN and (due to its fluorination) interacts strongly with PIC and PEN. The comparison of the binary mixtures of PEN:PIC, PFP:PIC, and PFP:PEN is thus very interesting since it offers a broad range of growth and mixing scenarios. Furthermore, in thin films the morphology is affected by growth kinetics. On Si covered with a native oxide layer PIC forms islands from the very first molecular layer (i.e., grows in Volmer−Weber growth mode),[33] which is different from PEN[34,35] and PFP[31,36] that grow in Stranski−Krastanov mode (layer-by-layer growth followed by the island formation). Therefore, the experiments presented here are relevant for a better understanding of structure formation in mixed thin films, primarily due to the effects of different growth modes and surface energies of the pristine molecules.

This paper is organized as follows. First, the structure of equimolar PFP:PIC mixtures grown at various temperatures including the molecular packing in the two different equimolar structures is discussed. Then PFP:PIC mixtures with varying mixing ratios are presented and compared to the structure of PEN:PIC mixtures to demonstrate how differences in mixed components lead to differences in mixing and growth behavior. Furthermore, the morphology of the mixed systems is shown, and complementary results of the X-ray absorption dichroism using near-edge X-ray absorption spectroscopy (NEXAFS) are presented supporting the X-ray diffraction experiments.

■ EXPERIMENTAL SECTION

Mixed thin films containing PIC (purchased from NARD Co. with 99.9% purity), PFP (purchased from Kanto Denka Kogyo Co. with 99% purity), and PEN (purchased from Sigma-Aldrich, 99.9% purity) were grown by coevaporation on Si substrates covered with a native oxide layer. The deposition rates were measured by a water-cooled quartz microbalance calibrated by X-ray reflectivity (XRR). To obtain the molar mixing ratios from the measured film volume we took the different molecular sizes into account determined from published crystal structures.[23,27,31] For PEN:PIC mixtures one series of samples with different molar mixing ratios of PEN:PIC (4:1, 1:1, 1:4) with a nominal thickness of 20 nm was grown at a substrate temperature of 297 K with a nominal deposition rate of 3 Å/min. After growth these samples were measured using a point detector for grazing incidence X-ray diffraction (GIXD) and XRR scans. An area detector (PILATUS 300 K

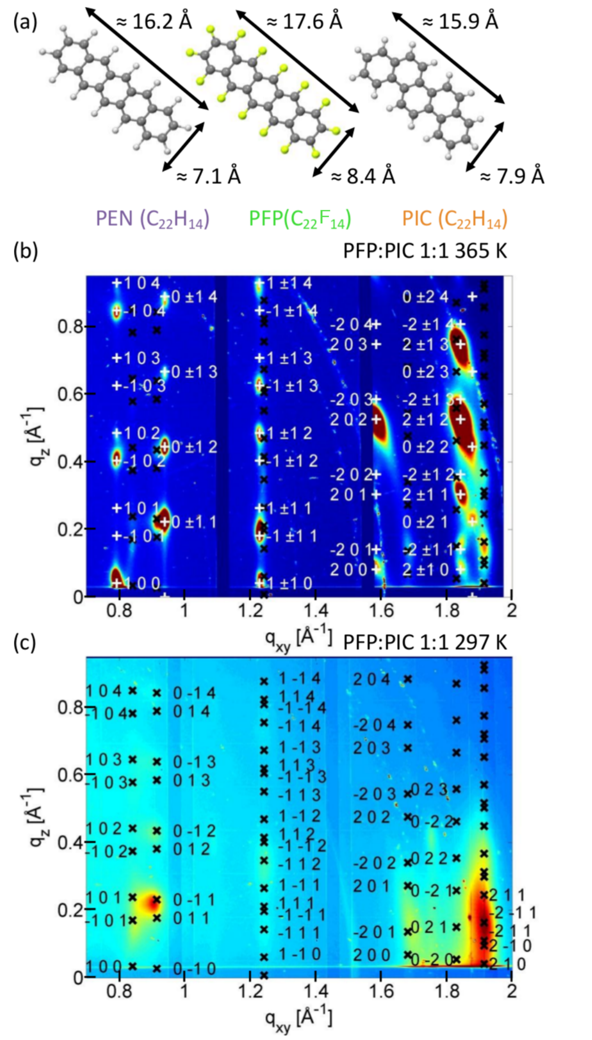

Figure 1. (a) Molecular structure of PEN, PFP, and PIC. For the molecular dimensions atomic distances from the crystal structures[23,27,30] and van der Waals radii were added. (b) Reciprocal space map of a PFP:PIC 1:1 mixture grown at 365 K. Simulated reflections consistent with the two distinct unit cells of structure I and structure II present at this growth temperature are marked with crosses (structure I, black; structure II, white). (c) Reciprocal space map of a PFP:PIC 1:1 mixture grown at room temperature (297 K). Black crosses mark potential reflections following from the unit cell parameters (i.e., not taking into account reflection extinction due to the unit cell symmetry). The weak peaks at q_{xy} = 1.09 and 1.754 Å^{-1} can be assigned to a very small amount of excess PFP.

with 487 × 619 pixels, 172 μm × 172 μm pixel size, and 20 bit dynamic range) was used for reciprocal space mapping with a wavelength of λ = 1.1271 Å at ID10 (ESRF, France). All these measurements were performed under vacuum in a beryllium dome to reduce air scattering. Preliminary measurements were performed at beamline X04SA[37] (SLS, Switzerland). The morphology was investigated by atomic force microscopy (AFM) using a JPK NanoWizard II.

Three different series of samples were prepared for PFP:PIC mixtures: The first series consists of samples with different mixing ratios of PFP:PIC (4:1, 2:1, 1:1, 1:2, 1:4) with a nominal thickness of 20 nm grown at 297 K with a nominal deposition rate of 3 Å/min. The same series of measurements was performed as for the PEN:PIC samples.

DOI: 10.1021/acs.jpcc.5b08866
J. Phys. Chem. C 2015, 119, 26339−26347

Additionally, the evolution of GIXD reciprocal space maps during growth of equimolar PFP:PIC mixtures was measured in situ and in real time.[38] The deposition rate for this sample series was 1.8 Å/min, and the substrate temperature for individual samples ranged from 310 to 365 K. Directly after the preparation process, the same set of X-ray measurements was performed as for the static samples post growth and in situ, in that case while kept at their preparation temperature. In order to determine the actual growth rate XRR data measured post growth were fitted with GenX[39] using a simple one-box model for the film, yielding growth rates between 1 and 1.8 Å/min. The unit cell parameters were determined by iteratively calculating q_{xy} and q_z values of the reflections from unit cell parameters using Matlab and manually adjusting them until an indexing of the peaks of the reciprocal space map was achieved. Following this, the unit cell parameters were fitted by a least-squares error routine. From the reciprocal space map the molecular packing in one of the equimolar polymorphs was determined. For this purpose the experimental peak intensities were extracted from the reciprocal space map, background was subtracted, and corrections as described in ref 40 were applied. The refinement was done by a genetic optimization algorithm supplied with Matlab. During the refinement, the molecules were treated as rigid bodies, only their positions within the unit cells and their orientations were fitted while the symmetry of the unit cell was kept consistent with the diffractogram. The structure factor of the molecular arrangement was calculated using atomic scattering factors taken from ref 41 and an isotropic Debye–Waller factor as a free parameter.

A third series of samples was prepared for NEXAFS and X-ray photoelectron spectroscopy (XPS) experiments to measure the average molecular tilt angle[42] and the stoichiometry for structurally different samples: PFP:PIC 1:1 mixtures grown at 310 (thickness 20 nm) and 373 K (thickness 6 and 20 nm) and pure PIC grown at 310 K were measured post growth at the HE-SGM beamline (BESSY II). Further information on the experimental details are presented in ref 43.

■ RESULTS

PFP:PIC Mixtures. Figure 1b shows a reciprocal space map of an equimolar PFP:PIC mixture grown at 365 K. The peaks are remarkably clear and sharp for a mixed system. All observed peaks do not correspond to known phases of the pure compounds. In addition, not all reflections occurring in Figure 1b can be described by one unit cell. Therefore, two unit cells are proposed corresponding to two different mixed structures (structure I and structure II). For details about the unit cell parameters, see Table 1. The unit cell volumes of both structures correspond roughly to the sum of a PIC and a PFP unit cell volume; however, the unit cell volume of structure I is 6% larger than that of structure II. The unit cells of both pure compounds contain 2 molecules; thus, to have a comparable density there has to be 4 molecules per unit cell in the mixed structures. The intensities of the peaks corresponding to structure II are much higher than for structure I, indicating that structure II is clearly dominating the mixture at high growth temperatures.

Table 1. Unit Cell Parameters of PIC, PFP, and the Two Different 1:1 Mixed Structures Determined at 365 K

	PIC[44]	PFP[31]	structure I	structure II
a [Å]	8.33	15.76	7.48 ± 0.03	7.93 ± 0.02
b [Å]	6.22	4.51	6.87 ± 0.06	6.69 ± 0.03
c [Å]	13.15	11.48	30.85 ± 0.46	28.35 ± 0.09
α [deg]	90	90	88.3 ± 0.7	90 ± 0.2
β [deg]	90	90.4	92.3 ± 0.4	92.9 ± 0.2
γ [deg]	90.25	90	90 ± 0.5	90 ± 0.2
volume [Å^3]	700	816	1582 ± 28	1493 ± 16

Equimolar PFP:PIC mixtures were investigated at different growth temperatures (310, 343, and 365 K) with a molecular flux resulting in a growth rate of 1.8 Å/min at 310 K. For 343 and 365 K, the growth rate is significantly reduced (45% at 365 K) due to reduced sticking. Surprisingly, the mixed film nucleates at 365 K, which is well above the maximal nucleation temperature of both PFP and PIC at such a low growth rate (~330 K), indicating that the intermixture is energetically significantly favored against the pure compounds, as similarly observed for mixtures of PFP and PEN where a significantly enhanced thermal stability was reported.[45] In the XRR data shown in Figure 2a the (001) Bragg peak of structure I at

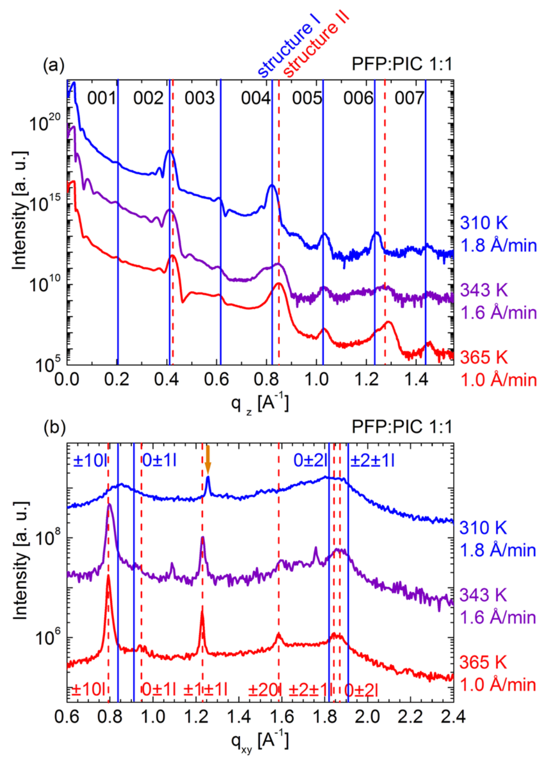

Figure 2. (a) XRR data for equimolar PFP:PIC films grown at different temperatures (offset for clarity). Vertical lines mark the positions of the Bragg peaks determined from the position of the (004) peak and scaled according to the indices (structure I, blue solid; structure II, red dashed). (b) GIXD data obtained from the same equimolar PFP:PIC films. The sharp peak at q_{xy} = 1.26 Å^{-1} (orange arrow) in the film grown at 310 K corresponds to the (110) reflection of a small PIC excess phase. Vertical lines indicate positions of Bragg reflections of structure I (blue continuous line) and structure II (red dashed line).

$q_z \approx 0.2$ Å^{-1} roughly one-half the q_z value of the first Bragg peak of PIC or PFP ($q_z \approx 0.4$ Å^{-1}) and higher odd orders are visible. The Bragg peaks with even indices are clearly superpositions of the Bragg peaks corresponding to the two mixed structures. For the film grown at 310 K, only the Bragg peaks of structure I are present in the reciprocal space map

DOI: 10.1021/acs.jpcc.5b08866
J. Phys. Chem. C 2015, 119, 26339–26347

(Figure 1c) as well as in the XRR data, while for the elevated temperatures the Bragg peaks of structure II and only shoulders resulting from structure I are observed in the XRR data. This indicates that structure I is present in all films, whereas structure II only occurs at elevated temperatures, being strongly dominating for samples prepared at 365 K. The Bragg peaks with odd indices in the XRR data can be uniquely attributed to structure I, since they are present at room temperature, and also the peak positions are consistent with the other Bragg peaks of structure I rather than with those of structure II (see lines in Figure 2a). The GIXD data (Figure 2b) exhibit peaks corresponding to the two different mixed structures. The very sharp and pronounced Bragg peaks of structure II at elevated temperatures indicate large coherent in-plane crystal size at these temperatures (the lower limit of coherent crystallite size obtained from fwhm of the ($\pm 10l$) reflections by the Scherrer formula: 53 (structure I, T = 310 K), 223 (structure II, T = 343 K), and 336 Å (structure II, T = 365 K)). Structure I is also present at elevated temperatures; however, no sharp and intense peaks are observed in GIXD. Thus, structure I is weakly ordered in-plane in contrast to structure II.

For structure II the molecular packing can be determined from the pronounced Bragg peaks in the reciprocal space map. The systematic absence of all ($\pm h0l$) reflections with odd l in the reciprocal space map (Figure 1b) as well as in the XRR data (Figure 2a) is an indication of a c-glide mirror plane perpendicular to the (010) direction with a gliding vector $c/2$. This implies that molecules of the same species are arranged at the same positions along the a axis, and the positions in the c direction differ by $c/2$, i.e., the unit cell consists of two molecular layers along the growth direction with 1 PIC and 1 PFP molecule per layer. Using these considerations the molecular packing was determined (see ref 46). The resulting molecular arrangement consisting of in-plane stacked alternating layers of the compounds is shown in Figure 3a, 3b, and 3d.

Structure I differs significantly from structure II since the (−101) as well as the (−201) reflections are present in the reciprocal space map (Figure 1) and all the (00l) reflections appear in the XRR (Figure 2). Furthermore, the strong (100) reflection in structure II indicating a highly modulated electron density profile along the a-axis is not observed in structure I. Since also the (0−10) reflection is absent, a segregation of the molecules along the a or the b axis can be ruled out. The weak (00l) reflections with odd indices in the XRR imply a small but detectable modulation of the projected electron density profile along the c axis with a periodicity of $c/2$. Since the PIC molecule has only one 2-fold rotational symmetry axis and the unit cell contains two PIC molecules that are separated by $c/2$ in the c direction, we propose that the modulation of the electron density is due to alternating orientation of the PIC molecules in neighboring molecular layers along the growth direction (i.e., along the c axis). On the basis of these observations we propose the crystal structure scheme sketched in Figure 3c for structure I. These determined structures are perfectly compatible with the X-ray dichroism analysis (NEXAFS), which revealed equivalent orientations of the individual molecular compounds in both structure I and structure II with tilt angles relative to the surface plane of ∼80° (full set of data and evaluation details in ref 46). The very good agreement with the XRD analysis further shows that no prominent amorphous regions exist in the samples, which would have reduced the average molecular orientation as

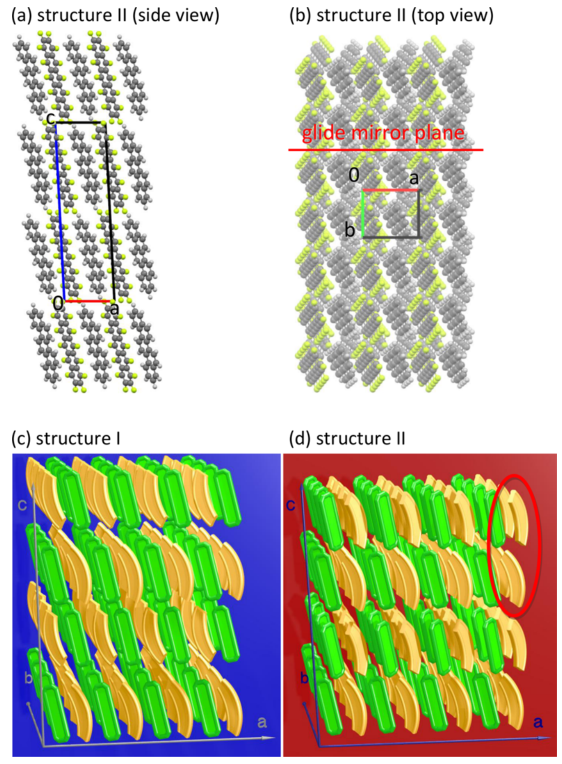

Figure 3. (a) Molecular packing in structure II determined from reciprocal space maps: view along the b axis and (b) view along the c axis. C, H, and F atoms are marked by dark gray, light gray, and yellow balls, respectively. The bottom layer has lighter shading. (c) Illustration of proposed packing in structure I. (d) Illustration of packing in structure II showing a 2D segregation of the compounds. Green, PFP; orange, PIC. Molecules in adjacent layers are oriented differently in plane (highlighted by red mark).

determined by NEXAFS.[43] The XPS measurements confirm the presumed stoichiometry of the mixtures.

For the equimolar mixture also the growth dynamics was investigated in situ and in real time. Figure 4 shows the evolution of the normalized peak intensity extracted from reciprocal space maps vs the film thickness. We observe different time evolutions of the intensity of peaks assigned to

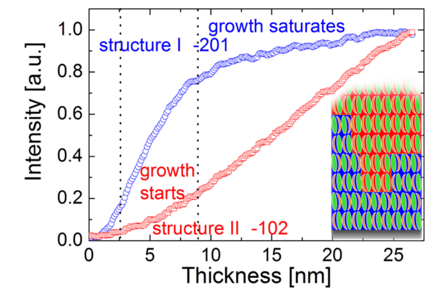

Figure 4. Thickness-dependent intensity evolution of the (−201) reflection of structure I and the (−102) reflection of structure II during growth at 365 K (blue circles, structure I; red squares, structure II) extracted from reciprocal space maps. Intensity values are normalized to the intensity of the final thickness. All other nonoverlapping reflections of the individual structures show the same thickness evolution. (Inset) Schematic of the growth behavior. Structure I is marked by a blue background and structure II by a red one. The first (second) dotted line indicates the start of the growth of structure II (saturation of growth of structure I).

DOI: 10.1021/acs.jpcc.5b08866
J. Phys. Chem. C 2015, 119, 26339−26347

the two mixed 1:1 structures at 365 K, clearly supporting the assumption of two different mixed structures. At the beginning, the peak intensities of structure I are growing rather fast while the ones belonging to structure II remain comparably weak, showing that structure I is dominating. After a thickness of 7.5 nm is reached the peak intensities of structure I increase slowly. In contrast, the intensities of the peaks assigned to structure II start evolving at 2.5 nm and from that point linearly increase over the residual thickness range, indicating that the nucleation of this structure starts after approximately 2 molecular layers. For equimolar films grown at lower temperature (310 K) only structure I is observed, and no indications for nucleation of structure II after a certain film thickness are found.

After clarification of the impact of growth temperature on PFP:PIC mixtures, we discuss now the structure of films grown at different mixing ratios. Figure 5a shows XRR data for the sample series with varying PFP:PIC mixing ratios grown at 300 K, which were investigated post growth. The (003) reflection at $q_z \approx 0.61$ Å^{-1} is visible even for nonequimolar mixtures, indicating the presence of structure I. For mixtures containing more PIC distinct peaks corresponding to pure PIC are observed. A prevalence of PFP results in shoulders at the positions of peaks for pure PFP. Most pronounced Laue and Kiessig oscillations are found in the PFP:PIC 1:1 mixture, indicating high out-of-plane ordering and low roughness. In the GIXD data (Figure 5b) weak and broad peaks for the equimolar mixture indicate small in-plane crystal grain size (see ref 46 for estimated coherent island sizes). No peaks related to known pure phases of PIC and PFP are present in the equimolar mixture. In nonequimolar mixtures, however, peaks corresponding to the pure phases of PFP and PIC as well as of the equimolar mixed structures are observed. In the 1:4 mixture, a comparatively sharp peak, related to structure II, is observed at $q_{xy} \approx 0.79$ Å^{-1}, which is rather unexpected since for equimolar mixtures this structure is only observed at elevated growth temperatures.

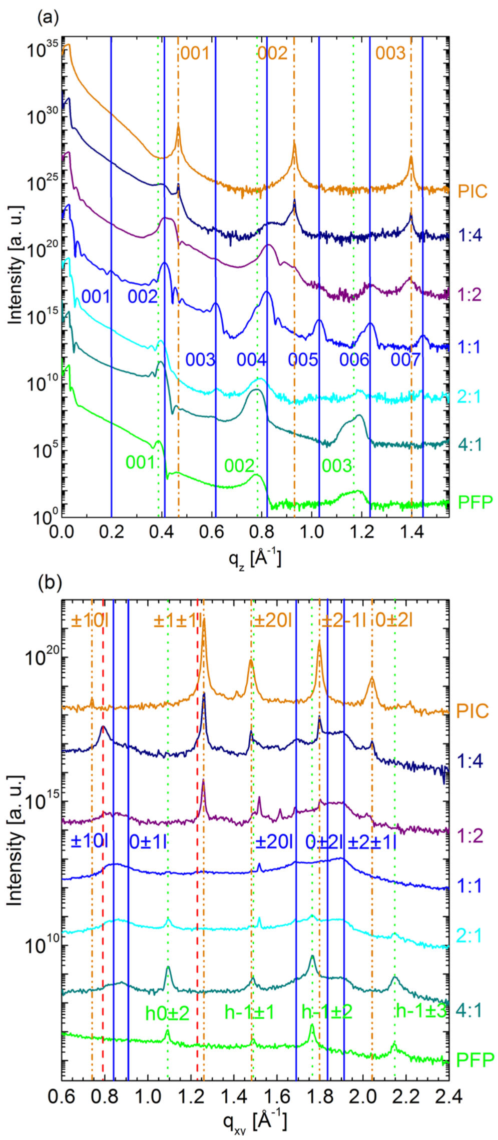

Figure 5. (a) XRR for PFP:PIC mixtures with various mixing ratios (offset for clarity), prepared at 297 K. (b) GIXD of the same PFP:PIC mixtures (offset for clarity). Vertical lines indicate positions of Bragg reflections of PFP (green dotted), PIC (orange dash dotted), PFP:PIC 1:1 structure I (blue solid), and structure II (red dashed).

The XRR and GIXD data indicate a coexistence of the 1:1 mixed structure I and the pure phases of the constituents. For the PIC-rich films additionally structure II is present.

PEN:PIC Mixtures. Motivated by the remarkable mixing behavior of PFP:PIC, we extended our investigations to blends of fluorine-free PEN and PIC which offer the opportunity to study how the favorable interaction between arenes and perfluoroarenes affects not only the mixing and ordering behavior but also the respective molecular arrangement in mixed films. A particularly interesting question is if a superlattice is formed for PEN:PIC blends as in the case of PFP:PIC or if the lack of a favorable interaction leads to a different ordering scheme. For PEN:PIC the XRR and GIXD data shown in Figure 6 reveal a continuous shift of all Bragg peaks between positions corresponding to PEN and PIC. The Bragg peaks in the GIXD are sharp and intense, indicating large in-plane crystal grain size in all films (see ref 46 for coherent crystallite sizes). This indicates mixing on the molecular level and the formation of a mixed crystal structure with a continuously changing composition and a random statistical distribution of the compounds. The pronounced Kiessig and Laue oscillations in the equimolar mixture show that the film is smooth and well ordered. Additionally, for the 1:4 mixture there are small Bragg reflections of pure PIC in both XRR and GIXD data. We attribute this phase separation and nucleation of excess PIC to limited intermixing between PIC and PEN. Since the reflections of the mixed structure in the 1:4 film are shifted toward positions of the PIC reflections compared to those in the 1:1 mixture, it can be concluded that the mixed structure in the 1:4 mixture is dominated by PIC despite the formation of a PIC excess phase. Moreover, experiments with a lower rate did not show a significant difference in the mixing behavior. This indicates that the nucleation of excess PIC is not merely a kinetical effect. The unit cell parameters are determined from reciprocal space maps (see Table 2). The absence of all ($\pm 10l$) and ($0\pm 1l$) reflections is also observed in pure PEN[47] and arises from herringbone stacking of the molecules. For pure PIC the herringbone stacking does not completely suppress these reflections due to the lower symmetry of PIC (see ($\pm 10l$) peak in GIXD data). Therefore, the absence of these reflections in the mixture implies that the PIC molecules are randomly rotated by 180° around their long axis within one crystallite.

DOI: 10.1021/acs.jpcc.5b08866
J. Phys. Chem. C 2015, 119, 26339−26347

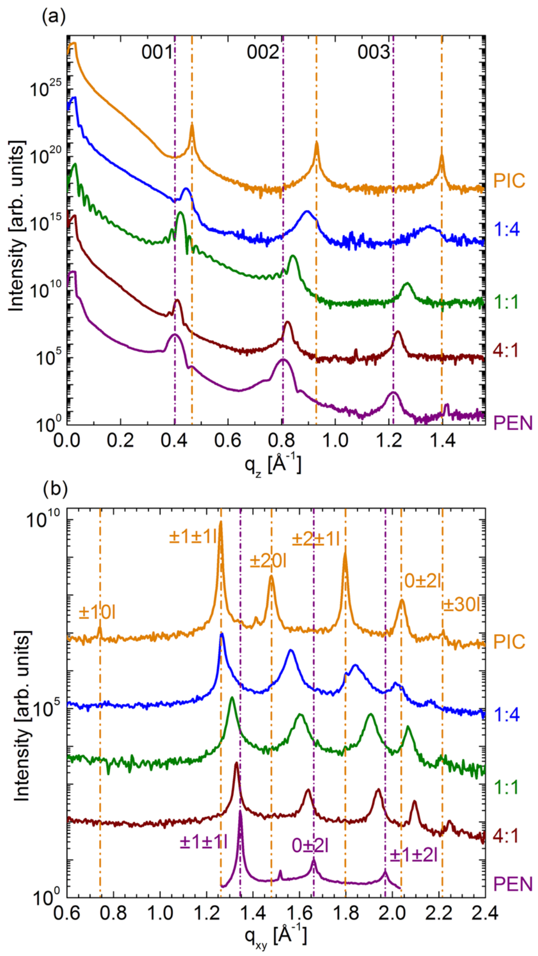

Figure 6. (a) XRR for PEN:PIC mixtures with various mixing ratios (offset for clarity). (b) GIXD of PEN:PIC mixtures with varying mixing ratio (offset for clarity).

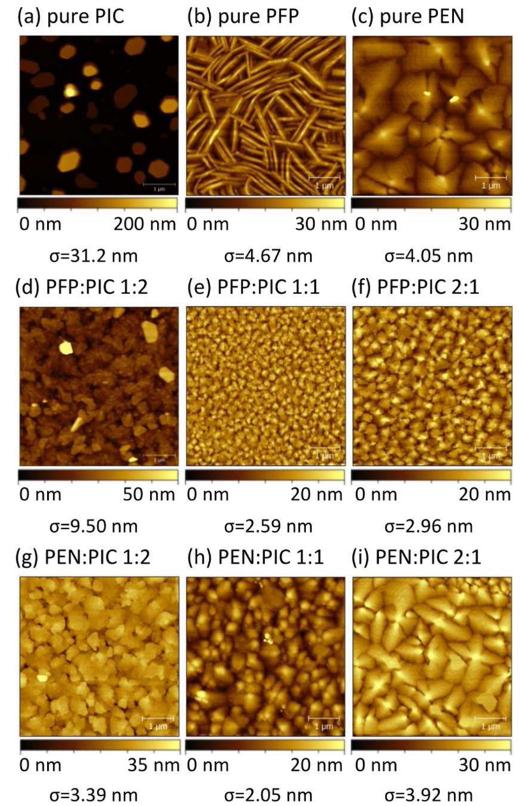

Figure 7. AFM images of (a) pure PIC, (b) pure PFP, (c) pure PEN, (d−f) PFP:PIC mixtures, and (g−i) PEN:PIC mixtures (area 5 μm × 5 μm) grown at a substrate temperature of 297 K. The root-mean-square roughness σ is given below the respective image.

Morphology. The AFM images (Figure 7) show typical island growth for pure PIC (Figure 7a) with sharp edges of the crystallites,[33] needle-like-shaped grains for pure PFP (Figure 7b),[31,36] and completely different morphologies for the mixed PFP:PIC films. For PFP:PIC 1:2 (Figure 7d) a mixed structure covers the whole substrate and clear PIC excess crystallites are found. The equimolar mixture (Figure 7e) is the smoothest one with small grains (∼280 nm) without any indication of excess phases. The 2:1 mixture (Figure 7f) has a similar morphology as the equimolar one but with a larger grain size of 500 nm. For PEN the AFM image (Figure 7c) shows Stranski−Krastanov growth[34,35] with an island base diameter of ∼1.7 μm. For the mixed PEN:PIC films, Stranski−Krastanov growth is also observed but with the island base diameter decreasing with the PIC fraction (1.3 μm for PEN:PIC 2:1, 0.8 μm for 1:1, and 0.65 μm for 1:2). The roughness σ (see Figure 7 for all values) is minimal for the equimolar mixture.

The fact that no pure PIC crystallites are observed is consistent with the scenario of complete mixing for the depicted mixing ratios. The AFM data illustrate the completely different growth modes of the pure compounds and supports the mixing and ordering behavior investigated by X-ray diffraction.

■ DISCUSSION

On the basis of earlier reports on mixtures of rodlike OSC molecules with high steric compatibility and the known strong interaction between fluorinated and nonfluorinated molecules

Table 2. Unit Cell Parameters of PIC, PEN:PIC Mixtures, and PEN[a]

	PIC[44]	PEN:PIC ratio 1:4	PEN:PIC ratio 1:1	PEN:PIC ratio 4:1	PEN[48]
a [Å]	8.33	8.04 ± 0.06	7.80 ± 0.03	7.73 ± 0.04	7.54
b [Å]	6.22	6.20 ± 0.06	6.03 ± 0.03	6.00 ± 0.05	5.92
c [Å]	13.15	14.15 ± 0.11	14.98 ± 0.12	15.55 ± 0.28	15.63
α [deg]	90	81.9 ± 2.6	88.7 ± 3.1	87.6 ± 1.6	87.2
β [deg]	90	85.4 ± 0.6	81.1 ± 0.9	80.4 ± 0.8	81.5
γ [deg]	90.25	90 ± 0.8	90 ± 0.8	90 ± 0.8	89.90
volume [Å^3]	681	696 ± 22	696 ± 14	710 ± 21	689

[a]Unit cell parameters of PEN are relabeled with respect to the original work[48] for better comparison with PIC.

DOI: 10.1021/acs.jpcc.5b08866
J. Phys. Chem. C 2015, 119, 26339−26347

(that favors intermixing) a molecular mixing and ordering behavior as observed in PFP:PEN[20,31,45] and PFP:DIP[21,49] is also expected for PFP:PIC. Indeed, PFP:PIC shows a mixing behavior resulting in a new mixed structure with a 1:1 molar ratio of the compounds which coexists with the pure crystal phases of the more abundant compound for nonequimolar mixtures as visualized in Figure 8a. For PFP:PIC the unit cell of the equimolar structure is approximately two times larger than the unit cell of the pure compound phases and contains 4 molecules (2 PFP and 2 PIC). In the case of structure II a 2D segregation of the species occurs. This finding is surprising, since due to the favorable interaction between fluorinated and nonfluorinated molecules a checkerboard-like arrangement of the molecules is expected for the molecules in the 1:1 structure as presumed for structure I viewed along the *b* axis, PFP:PEN, and PFP:DIP and observed in single crystals.[16] Furthermore, in structure I only a short-ranged in-plane ordering is observed, whereas PFP:PEN and PFP:DIP are well ordered in plane.

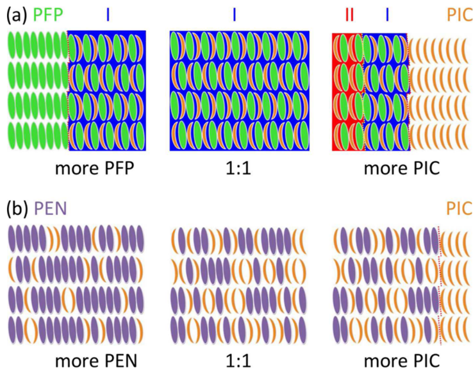

Figure 8. (a) Schematic of mixing behavior of PFP:PIC: equimolar structure and pure excess phases of the major compound at 297 K. Structure I (blue background) is present in all mixtures; structure II (red background) is only observed for high PIC fractions. (b) Schematic of mixing behavior of PEN:PIC: continuous intermixing and pure PIC excess phase for high PIC concentrations.

This behavior can be related to the molecular structure of PIC that differs qualitatively from PFP, PEN, and DIP due to its lower symmetry (only one 2-fold rotational axis) and the fact that the long axis of PIC is terminated by only one H atom, whereas there are two atoms at each end for PFP, PEN, and DIP. Due to the strong face-to-face interaction between fluorinated and nonfluorinated molecules a face-to-face arrangement of the PIC and PFP molecules in one layer is preferred. On the other hand, the H atom in one layer interacts favorably with one of the two F atoms of the adjacent layer. Therefore, it can be expected that adjacent layers are arranged in a way that the interlayer interaction is maximized. The molecular packing determined for structure II shows, indeed, a rather short distance between H and F atoms (<2 Å). A 2D segregation of the compounds takes place in this structure. As shown in Figure 3d, the molecular planes in the vertically adjacent layers are mutually tilted along the *c* axis to maximize the interlayer attraction. From these considerations it is intuitive that due to their shape the molecules of one species in adjacent layers can be placed on top of each other while establishing an energetically favorable structure. This segregation differs from 2D segregation known from the charge transfer salt TTF:TCNQ.[50] There only a strong face-to-face attraction of like molecules occurs since TTF and TCNQ differ significantly in their molecular structure, and therefore, like molecules are arranged perfectly face-to-face. The molecular packing in structure I of PFP:PIC, however, differs significantly from structure II. In structure I the different orientation of the PIC molecules (see Figure 3) can also be rationalized by the interlayer interactions. Due to the two different possible orientations of the PIC molecules in similar in-plane arrangements there are two different configurations with different arrangements of the interacting atoms. If there is lower compatibility for stacking two layers of the same arrangements as different ones, the molecules in the adjacent layers cannot be coplanar but their molecular planes have to be oriented oppositely. In contrast to structure II and other mixtures like PFP:PEN or PFP:DIP there is only a short-ranged in-plane ordering, although PFP and PIC are highly compatible and interact attractively due to the different chemical composition. Furthermore, the unit cell volume of this structure is larger by 6%. This difference in the ordering behavior could be caused by the interplay between the chemical composition, steric properties, and difference in the shape of the molecules that results in an energetically unfavorable structure. Since the unit cell of both equimolar structures is extended over two molecular layers, the formation of a unit cell requires the arrangement of molecules in both layers. Therefore, it can be expected that in a nonequilibrium process like growth a metastable structure might form. Also, the real-time evolution (Figure 4) can be explained by these factors. During the nucleation of the first monolayer there is no interaction with other monolayers. Therefore, in this layer the in-plane arrangement is not affected by interlayer interactions and structure I is preferred. In subsequent layers these interactions become more important, leading to a preferred nucleation of structure II, which seems to be energetically favorable in this case. The high maximal nucleation temperature of PFP:PIC shows that the equimolar structures are more stable than the pure phases due to the strong favorable interaction between PFP and PIC. As demonstrated, growing an equimolar mixed film at a temperature above the maximal nucleation temperatures of the pure phases therefore is a possible route to eliminate formation of excess pure phases connected to minimal deviations in the ratio of the evaporation rates.

The equimolar PEN:PIC mixture forms a mixed structure with random distribution of the molecules on lattice sites. Due to the high steric compatibility the mixed system shows good in- and out-of-plane ordering. The lattice parameters of this mixture change continuously with varying mixing ratio similar to the mixing behavior of PEN:DIP.[22] This mixing behavior is visualized in Figure 8b and clearly differs from the mixing behavior of the PFP:PIC mixtures (Figure 8a). While in PEN:DIP the large sterical incompatibility results in an almost completely vanishing long-range in-plane order, the difference in the shape between PEN and PIC only slightly reduces the in-plane ordering compared to the pure compounds. Since there is only minimal preferred interaction between PEN and PIC compared to that between the same species due to the absence of fluorine atoms, effects observed in PFP:PIC mixtures driven by strong PFP−PIC interaction are not observed. The limited intermixing of PIC in the PEN:PIC mixtures is comparable to the mixing behavior reported for thin film mixtures of α-sexithiophene and p-sexiphenyl (6T:6P),[15] where in 6T-rich films a coexistence of a pure 6T phase and a 6P-rich mixed phase is assumed. This phase separation is explained by the shorter conjugated core of 6T compared to 6P that allows an

DOI: 10.1021/acs.jpcc.5b08866
J. Phys. Chem. C 2015, 119, 26339−26347

intercalation of 6T molecules in a 6P-rich phase but causes a too small lattice spacing in a 6T-rich phase for intercalation of 6P. Our results for PEN:PIC support this model since PIC is slightly shorter than PEN but contrary to the assumptions for 6T:6P show that the excess phase of the shorter PIC molecules coexists with a PIC-rich mixed phase in films with high PIC fraction.

■ CONCLUSION

Two molecular mixed systems with structurally similar arene compounds but very different molecular interactions were investigated. We observed two distinct 1:1 polymorphs (structure I and II) for equimolar mixtures of PFP:PIC with unit cells extended over two molecular layers. For structure II, the interplay between the chemical composition, steric properties, and the intramolecular arrangement of the atoms important for intermolecular interactions leads to a superlattice with a 2D segregation of the compounds. These factors also affect the ordering behavior in the two polymorphs. Structure II shows large in-plane order, while structure I is only weakly ordered in-plane but nucleates more easily directly on the Si oxide substrate. Thus, the two polymorphs show different growth behavior and temperature dependence. At low temperatures only structure I is observed, while at high temperatures structure I only grows at the beginning of the growth and later structure II dominates. Therefore, it can be concluded that structure I corresponds to a thin film phase which preferably nucleates in the first few molecular layers on the substrate. Structure II seems to be preferred in the bulk, and a transition from growth of structure I to structure II takes place during growth at higher temperatures (343 K and above). Due to the strong, favorable interaction between PFP and PIC, the equimolar structure can be grown at higher temperatures, at which pure compounds already do not nucleate on Si oxide. The deposition of perfectly equimolar mixtures at elevated temperatures might offer new perspectives for applications requiring exact stoichiometries. In contrast, for PEN:PIC due to the lack of specific arene−perfluoroarene interactions, no such surprising effects occur and the effect of the slightly different molecular structure on the mixing and ordering behavior can be explained merely by steric issues, i.e., the length difference. PEN:PIC forms crystals with unit cell parameters monotonously changing with the molar concentrations between those of PEN and PIC. The position of molecular species within the crystal lattice is statistical. For high PIC concentrations, due to the length difference of PEN and PIC, a phase separation of surplus PIC molecules occurs, which corresponds to a limited intermixing of the two compounds.

Our results provide new insights into the mixing and ordering behavior as well as the molecular arrangement in binary mixtures that critically affect physical properties relevant for applications.

■ ASSOCIATED CONTENT

Ⓢ Supporting Information

The Supporting Information is available free of charge on the ACS Publications website at DOI: 10.1021/acs.jpcc.5b08866.

Details about the determination of the molecular packing in structure II, crystal grain sizes, NEXAFS, and XPS data (PDF)

Crystallographic data for structure II in CIF format (CIF)

■ AUTHOR INFORMATION

Corresponding Author

*E-mail: frank.schreiber@uni-tuebingen.de.

Notes

The authors declare no competing financial interest.

■ ACKNOWLEDGMENTS

X-ray diffraction experiments were performed on the ID10 beamline at the European Synchrotron Radiation Facility (ESRF), Grenoble, France. We are grateful to Oleg Konovalov at ESRF for providing assistance in using beamline ID10. We acknowledge the Paul Scherrer Institut, Villigen, Switzerland, for provision of synchrotron radiation beamtime at beamline X04SA[37] of the SLS and would like to thank Nicola Casati for assistance. Furthermore, we acknowledge the Helmholtz-Zentrum Berlin (electron storage ring BESSY II) for provision of synchrotron radiation at beamline HE-SGM. K.B. acknowledges support of the Deutsche Forschungsgemeinschaft (BR 4869_1-1). T.B. and G.W. acknowledge support of the Deutsche Forschungsgemeinschaft (Grant SFB 1083, TP A2). J.N. acknowledges support from the Project CEITEC (Grant No. CZ.1.05/1.1.00/02.0068) from the European Regional Development Fund.

■ REFERENCES

(1) Brütting, W.; Adachi, C. In *Physics of Organic Semiconductors*, 2nd ed.; Brütting, W., Ed.; Wiley VCH-Verlag: Weinheim, 2012.

(2) Sirringhaus, H. 25th Anniversary Article: Organic Field-Effect Transistors: The Path Beyond Amorphous Silicon. *Adv. Mater.* **2014**, *26*, 1319−1335.

(3) Jou, J.-H.; Kumar, S.; Agrawal, A.; Li, T.-H.; Sahoo, S. Approaches for Fabricating High Efficiency Organic Light Emitting Diodes. *J. Mater. Chem. C* **2015**, *3*, 2974−3002.

(4) Thejo Kalyani, N.; Dhoble, S. Organic Light Emitting Diodes: Energy Saving Lighting Technology-A Review. *Renewable Sustainable Energy Rev.* **2012**, *16*, 2696−2723.

(5) Cao, W.; Xue, J. Recent Progress in Organic Photovoltaics: Device Architecture and Optical Design. *Energy Environ. Sci.* **2014**, *7*, 2123−2144.

(6) Yu, J.; Zheng, Y.; Huang, J. Towards High Performance Organic Photovoltaic Cells: A Review of Recent Development in Organic Photovoltaics. *Polymers* **2014**, *6*, 2473−2509.

(7) Hesse, R.; Hofberger, W.; Bässler, H. Absorption Spectra of Disordered Solid Tetracene and Pentacene. *Chem. Phys.* **1980**, *49*, 201−211.

(8) Yoshida, Y.; Takiguchi, H.; Hanada, T.; Tanigaki, N.; Han, E.-M.; Yase, K. Control of Growth Mechanism and Optical Properties of p-Sexiphenyl Thin Films on Ionic Crystal Substrates. *J. Cryst. Growth* **1999**, *198−199*, 923−928.

(9) Kolata, K.; Breuer, T.; Witte, G.; Chatterjee, S. Molecular Packing Determines Singlet Exciton Fission in Organic Semiconductors. *ACS Nano* **2014**, *8*, 7377−7383.

(10) Opitz, A.; Wagner, J.; Brütting, W.; Hinderhofer, A.; Schreiber, F. Molecular Semiconductor Blends: Microstructure, Charge Carrier Transport, and Application in Photovoltaic Cells. *Phys. Status Solidi A* **2009**, *206*, 2683−2694.

(11) Heutz, S.; Sullivan, P.; Sanderson, B.; Schultes, S.; Jones, T. Influence of Molecular Architecture and Intermixing on the Photovoltaic, Morphological and Spectroscopic Properties of CuPcC_{60} Heterojunctions. *Sol. Energy Mater. Sol. Cells* **2004**, *83*, 229−245.

(12) Schreiber, F. Organic Molecular Beam Deposition: Growth Studies Beyond the First Monolayer. *Phys. Status Solidi A* **2004**, *201*, 1037−1054.

(13) Kitaigorodsky, A. In *Mixed Crystals*; Cordona, M., Ed.; Springer: Berlin, Heidelberg, 1984.

DOI: 10.1021/acs.jpcc.5b08866
J. Phys. Chem. C 2015, 119, 26339−26347

(14) Hinderhofer, A.; Schreiber, F. Organic-Organic Heterostructures: Concepts and Applications. *ChemPhysChem* **2012**, *13*, 628−643.

(15) Vogel, J. O.; Salzmann, I.; Duhm, S.; Oehzelt, M.; Rabe, J. P.; Koch, N. Phase-Separation and Mixing in Thin Films of Co-deposited Rod-Like Conjugated Molecules. *J. Mater. Chem.* **2010**, *20*, 4055−4066.

(16) Bacchi, S.; Benaglia, M.; Cozzi, F.; Demartin, F.; Filippini, G.; Gavezzotti, A. X-ray Diffraction and Theoretical Studies for the Quantitative Assessment of Intermolecular Arene-Perfluoroarene Stacking Interactions. *Chem. - Eur. J.* **2006**, *12*, 3538−3546.

(17) Collings, J. C.; Roscoe, K. P.; Thomas, R. L.; Batsanov, A. S.; Stimson, L. M.; Howard, J. A. K.; Marder, T. B. Arene-Perfluoroarene Interactions in Crystal Engineering. Part 3. Single-Crystal Structures of 1:1 Complexes of Octafluoronaphthalene with Fused-Ring Polyaromatic Hydrocarbons. *New J. Chem.* **2001**, *25*, 1410−1417.

(18) Coates, G. W.; Dunn, A. R.; Henling, L. M.; Ziller, J. W.; Lobkovsky, E. B.; Grubbs, R. H. Phenyl-Perfluorophenyl Stacking Interactions: Topochemical [2 + 2] Photodimerization and Photopolymerization of Olefinic Compounds. *J. Am. Chem. Soc.* **1998**, *120*, 3641−3649.

(19) Reichenbächer, K.; Süss, H. I.; Hulliger, J. Fluorine in Crystal Engineering-"the Little Atom that Could. *Chem. Soc. Rev.* **2005**, *34*, 22−30.

(20) Hinderhofer, A.; Frank, C.; Hosokai, T.; Resta, A.; Gerlach, A.; Schreiber, F. Structure and Morphology of Coevaporated Pentacene-Perfluoropentacene Thin Films. *J. Chem. Phys.* **2011**, *134*, 104702.

(21) Reinhardt, J. P.; Hinderhofer, A.; Broch, K.; Heinemeyer, U.; Kowarik, S.; Vorobiev, A.; Gerlach, A.; Schreiber, F. Structural and Optical Properties of Mixed Diindenoperylene-Perfluoropentacene Thin Films. *J. Phys. Chem. C* **2012**, *116*, 10917−10923.

(22) Aufderheide, A.; Broch, K.; Novák, J.; Hinderhofer, A.; Nervo, R.; Gerlach, A.; Banerjee, R.; Schreiber, F. Mixing-Induced Anisotropic Correlations in Molecular Crystalline Systems. *Phys. Rev. Lett.* **2012**, *109*, 156102.

(23) De, A.; Ghosh, R.; Roychowdhury, S.; Roychowdhury, P. Structural Analysis of Picene, $C_{22}H_{14}$. *Acta Crystallogr., Sect. C: Cryst. Struct. Commun.* **1985**, *41*, 907−909.

(24) Mitsuhashi, R.; Suzuki, Y.; Yamanari, Y.; Mitamura, H.; Kambe, T.; Ikeda, N.; Okamoto, H.; Fujiwara, A.; Yamaji, M.; Kawasaki, N.; et al. Superconductivity in Alkali-Metal-Doped Picene. *Nature* **2010**, *464*, 76−79.

(25) Kawasaki, N.; Kubozono, Y.; Okamoto, H.; Fujiwara, A.; Yamaji, M. Trap States and Transport Characteristics in Picene Thin Film Field-Effect Transistor. *Appl. Phys. Lett.* **2009**, *94*, 043310.

(26) Koch, N. Organic Electronic Devices and Their Functional Interfaces. *ChemPhysChem* **2007**, *8*, 1438−1455.

(27) Campbell, R. B.; Robertson, J. M.; Trotter, J. The Crystal and Molecular Structure of Pentacene. *Acta Crystallogr.* **1961**, *14*, 705−711.

(28) Wang, G.; Luo, Y.; Beton, P. H. High Mobility Organic Transistors Fabricated from Single Pentacene Microcrystals Grown on a Polymer Film. *Appl. Phys. Lett.* **2003**, *83*, 3108−3110.

(29) Troisi, A. Charge Transport in High Mobility Molecular Semiconductors: Classical Models and New Theories. *Chem. Soc. Rev.* **2011**, *40*, 2347−2358.

(30) Sakamoto, Y.; Suzuki, T.; Kobayashi, M.; Gao, Y.; Fukai, Y.; Inoue, Y.; Sato, F.; Tokito, S. Perfluoropentacene: High-Performance p-n Junctions and Complementary Circuits with Pentacene. *J. Am. Chem. Soc.* **2004**, *126*, 8138−8140.

(31) Salzmann, I.; Duhm, S.; Heimel, G.; Rabe, J. P.; Koch, N.; Oehzelt, M.; Sakamoto, Y.; Suzuki, T. Structural Order in Perfluoropentacene Thin Films and Heterostructures with Pentacene. *Langmuir* **2008**, *24*, 7294−7298.

(32) Frank, C.; Novák, J.; Gerlach, A.; Ligorio, G.; Broch, K.; Hinderhofer, A.; Aufderheide, A.; Banerjee, R.; Nervo, R.; Schreiber, F. Real-Time X-ray Scattering Studies on Temperature Dependence of Perfluoropentacene Thin Film Growth. *J. Appl. Phys.* **2013**, *114*, 043515.

(33) Kurihara, R.; Hosokai, T.; Kubozono, Y. Growth and Structure of Picene Thin Films on SiO_2. *Mol. Cryst. Liq. Cryst.* **2013**, *580*, 83−87.

(34) Heringdorf zu, F. M.; Reuter, M. C.; Tromp, R. M. Growth Dynamics of Pentacene Thin Films. *Nature (London, U. K.)* **2001**, *412*, 517−520.

(35) Ruiz, R.; Choudhary, D.; Nickel, B.; Toccoli, T.; Chang, K.; Mayer, A. C.; Clancy, P.; Blakely, J. M.; Headrick, R. L.; Iannotta, S.; et al. Pentacene Thin Film Growth. *Chem. Mater.* **2004**, *16*, 4497−4508.

(36) Kowarik, S.; Gerlach, A.; Hinderhofer, A.; Milita, S.; Borgatti, F.; Zontone, F.; Suzuki, T.; Biscarini, F.; Schreiber, F. Structure, morphology, and Growth Dynamics of Perfluoro-Pentacene Thin Films. *Phys. Status Solidi RRL* **2008**, *2*, 120−122.

(37) Willmott, P. R.; Meister, D.; Leake, S. J.; Lange, M.; Bergamaschi, A.; Böge, M.; Calvi, M.; Cancellieri, C.; Casati, N.; Cervellino, A.; et al. The Materials Science Beamline Upgrade at the Swiss Light Source. *J. Synchrotron Radiat.* **2013**, *20*, 667−682.

(38) Ritley, K. A.; Krause, B.; Schreiber, F.; Dosch, H. A Portable Ultrahigh Vacuum Organic Molecular Beam Deposition System for *In Situ* X-ray Diffraction Measurements. *Rev. Sci. Instrum.* **2001**, *72*, 1453−1457.

(39) Björck, M.; Andersson, G. GenX: An Extensible X-ray Reflectivity Refinement Program Utilizing Differential Evolution. *J. Appl. Crystallogr.* **2007**, *40*, 1174−1178.

(40) Mannsfeld, S. C. B.; Virkar, A.; Reese, C.; Toney, M. F.; Bao, Z. Precise Structure of Pentacene Monolayers on Amorphous Silicon Oxide and Relation to Charge Transport. *Adv. Mater.* **2009**, *21*, 2294−2298.

(41) Waasmaier, D.; Kirfel, A. New Analytical Scattering-Factor Functions for Free Atoms and Ions. *Acta Crystallogr., Sect. A: Found. Crystallogr.* **1995**, *51*, 416−431.

(42) Broch, K.; Bürker, C.; Dieterle, J.; Krause, S.; Gerlach, A.; Schreiber, F. Impact of Molecular Tilt Angle on the Absorption Spectra of Pentacene:Perfluoropentacene Blends. *Phys. Status Solidi RRL* **2013**, *7*, 1084−1088.

(43) Breuer, T.; Klues, M.; Witte, G. Characterization of Orientational Order in π-conjugated Molecular Thin Films by NEXAFS. *J. Electron Spectrosc. Relat. Phenom.* **2015**, *204*, 102−115.

(44) Hosokai, T.; Hinderhofer, A.; Vorobiev, A.; Lorch, C.; Watanabe, T.; Koganezawa, T.; Gerlach, A.; Yoshimoto, N.; Kubozono, Y.; Schreiber, F. In Situ Structural Characterization of Picene Thin Films by X-ray Scattering: Vacuum versus O_2 Atmosphere. *Chem. Phys. Lett.* **2012**, *544*, 34−38.

(45) Breuer, T.; Witte, G. Thermally Activated Intermixture in Pentacene-Perfluoropentacene Heterostructures. *J. Chem. Phys.* **2013**, *138*, 114901.

(46) Supplemental Information.

(47) Yoshida, H.; Sato, N. Grazing-Incidence X-ray Diffraction Study of Pentacene Thin Films with the Bulk Phase Structure. *Appl. Phys. Lett.* **2006**, *89*, 101919.

(48) Nabok, D.; Puschnig, P.; Ambrosch-Draxl, C.; Werzer, O.; Resel, R.; Smilgies, D.-M. Crystal and Electronic Structures of Pentacene Thin Films from Grazing-Incidence X-ray Diffraction and First-Principles Calculations. *Phys. Rev. B: Condens. Matter Mater. Phys.* **2007**, *76*, 235322.

(49) Broch, K.; Gerlach, A.; Lorch, C.; Dieterle, J.; Novák, J.; Hinderhofer, A.; Schreiber, F. Structure Formation in Perfluoropentacene:Diindenoperylene Blends and Its Impact on Transient Effects in the Optical Properties Studied in Real-Time During Growth. *J. Chem. Phys.* **2013**, *139*, 174709.

(50) Kistenmacher, T. J.; Phillips, T. E.; Cowan, D. O. The Crystal Structure of the 1:1 Radical Cationradical Anion Salt of 2.2′-bis-l,3-dithiole (TTF) and 7.7,8.8-Tetracyanoquinodimethane (TCNQ). *Acta Crystallogr., Sect. B: Struct. Crystallogr. Cryst. Chem.* **1974**, *30*, 763−768.

DOI: 10.1021/acs.jpcc.5b08866
J. Phys. Chem. C 2015, 119, 26339−26347